Identification of unsteady effects in the flow through a centrifugal fan using CFD/CAA methods

BALAZS PRITZ[1]
MATTHIAS PROBST[1]
PIOTR WIŚNIEWSKI[2*]
SŁAWOMIR DYKAS[2]
MIROSŁAW MAJKUT[2]
KRYSTIAN SMOŁKA[2]

Institute of Thermal Turbomachinery, Karlsruhe Institute of Technology, Kaiserstraße 12 D-76131 Karlsruhe, Germany
Department of Power Engineering and Turbomachinery, Silesian University of Technology, Poland

Abstract Besides centrifugal pumps, centrifugal fans are the most com-mon turbomachines used in technical applications. They are commonly used in power engineering systems, such as heat engines and chillers, heating, ven-tilation, and air conditioning systems, supply and exhaust air systems. They are also used as machines consuming final energy (electricity). Therefore, any improvement in their efficiency affects the efficiency of energy genera-tion and the level of electricity consumption. Many efforts have been made so far to find the most efficient numerical method of modelling flows in fans. However, only a few publications focus on the unsteadiness that may have an impact on device efficiency and noise generation. This paper presents an attempt to identify unsteadiness in the flow through a centrifugal fan by means of computational fluid dynamics and computational aeroacoustics methods. The works were performed using the Ansys CFX commercial soft-ware and the results of numerical studies are compared with experimental data.

Keywords: Centrifugal fan; CFD; CAA

Acronyms

BPF	–	blade passing frequency
CAA	–	computational aeroacoustics
CFD	–	computational fluid dynamics
FFT	–	fast Fourier transform
LES	–	large eddy simulation
PIV	–	particle image velocimetry
SAS	–	scale adaptive simulation

1 Introduction

Centrifugal fans are commonly used in many technical applications in almost any industrial sector, such as the power, environmental, chemical, aviation or space industry. Therefore, centrifugal fans need to be developed further to achieve high efficiency, save energy and reduce noise emis-sions. The latest design methods are based on computationa fluid dynamics (CFD) simulations and aeroacoustic analysis [1–6]. At the same time, ex-perimental measurements are developed using state-of-the-art techniques, such as particle image velocimetry (PIV) [7,8]. The novel experimental flow and noise measurements provide data enabling a deeper understanding of the flow phenomena and a better selection of the CFD/CAA models for simulations.

The noise emitted by a turbomachine such as a centrifugal fan can be divided [3, 9] into external noise carried with the flow leaving the machine and internal noise coming through the casing. Most of the noise generating mechanisms in fans are now well-recognized [10].

Computational fluid dynamics (CFD) and computational aeroacoustics (CAA) analyses were performed within this study to identify the noise sources in a backwards-curved centrifugal fan with a vaneless volute diffuser. According to the literature survey, a few main reasons are favouring aerodynamic noise generation. The first is the discrete frequency noise arising due to the interaction between the fan moving and stationary parts. The fundamental component of the discrete frequency noise, depending on the rotor rotational speed and the number of rotor blades, is called the blade passing frequency (BPF). The entire range of the discrete frequency noise is tonal noise, i.e. a noise audible to the human ear. The second type of aerodynamic noise is broadband noise, caused by the formation of vortices due to turbulent effects in the flow [11, 12]. This noise has usually a high

frequency, much above 1 kHz. Another type of noise is generated by infra-sound acoustic waves of a frequency lower than 20 Hz. This noise usually has its origin in the vibration of solid bodies, such as casings, pipelines, etc., and is emitted outside the machine. Aeroacoustic sources of that noise may exist, e.g. in big open axial rotor fans with a low number of blades spinning with a low rotational speed or as Helmholtz modes of the piping system [13].

It is known that tonal noise can be induced by aerodynamic forces aris-ing, for example, due to non-uniform inlet conditions, non-uniform rotor geometry, vortex shedding, inviscid vortices caused by inertial forces or even a stall. The rotating stall is a complex phenomenon that occurs at low flow rates, contributing to a change in the blade incident flow angle. A stall vortex is formed on the suction side of the blade turning around the rotor at about ~40% of the rotor rpm, and the direction is opposite to the motion of the blades. This phenomenon causes unsteady blade forces and consequently generates noise and vibrations. Rotating stall and surge instabilities are the key problems for the achievement of proper working conditions of a centrifugal fan and a detailed understanding of these phe-nomena is very important. They may occur during different off-design work-ing conditions, e.g. due to a sudden increase in the rotational speed or flow throttling [2, 9].

The research on the rotating stall initiation and suppression concerns compressors used in aero-propulsion applications or gas turbines [14]. A ro-tating stall can cause dangerous structural excitation and eventual destruc-tion of the compressor. Machines with a lower pressure rise, such as the fan investigated herein, can be operated safely for extended periods even in the presence of a rotating stall. However, due to the performance deterioration and noise generation associated with the rotating stall, operation under this flow regime is undesirable.

Because aeroacoustic noise is dependent on the aerodynamics due to the unsteady pressure fluctuations in the fan, a decision was made to quantify the noise sources by conducting a detailed transient CFD analysis. Usu-ally, the next step after CFD simulations is the conversion of the flow simulation results using the Lighthill acoustic analogy and the Ffowcs-Williams/Hawkings extension [15, 16]. The main focus of the analysis pre-sented herein is to identify the acoustic sources, and not noise propagation outside. To this end, the Lighthill stress tensor at the outlet surface has to be extracted from the CFD calculations so that it can be used in the wave equation for modelling the propagation of sound outside the fan.

2 Research methodology

2.1 Device under investigation

The investigated device is a backward curved centrifugal fan with a vaneless diffuser presented in Fig. 1. The fan was designed for a volume flow rate of $\dot{V}$ = 0.15 m^3/s, and a total pressure rise of Δp = 390 Pa at 1500 rpm. The fan impeller with nine blades (z = 9) and an outer diameter of 0.325 m rotates for the first series of experimental and numerical investigations, however, at 600 rpm due to the safety of the glued construction. The current version of the test fan is prepared for PIV measurements within blade channels.

The measured and calculated efficiency for the nominal load is about η = 72%. No acoustic measurements have been made yet. The blade pass-ing frequency (BPF) for the geometry of the nine-blade centrifugal fan considered herein should total: BPF = $z \cdot n/60 = 9 \cdot 600/60 = 90$ Hz.

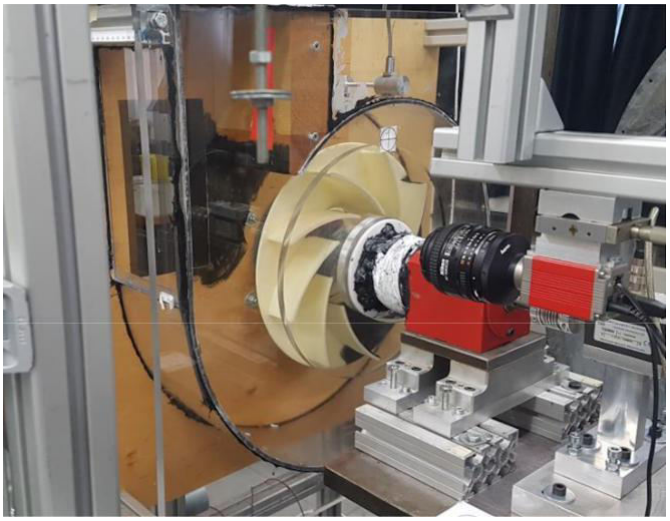

Figure 1: Centrifugal fan test rig at the Karlsruhe Institute of Technology (KIT).

2.2 Experimental test rig

The test rig experimental setup is illustrated in Fig. 2. The impeller is assembled out of two parts. The backwards-curved blades with a two-dimensional design and the shroud are manufactured by means of fast-

prototyping. The hub, the spiral casing as well as the sidewall of the hous-ing hub are made of acrylic glass for optical accessibility. In order to record the performance curve of the centrifugal fan, pressure values are taken up-stream and downstream of the fan to determine the total pressure increase. Pressure measurement in the straight pipe section ($pV\dot{}$) gives the volume flow rate according to DIN EN ISO 5167.

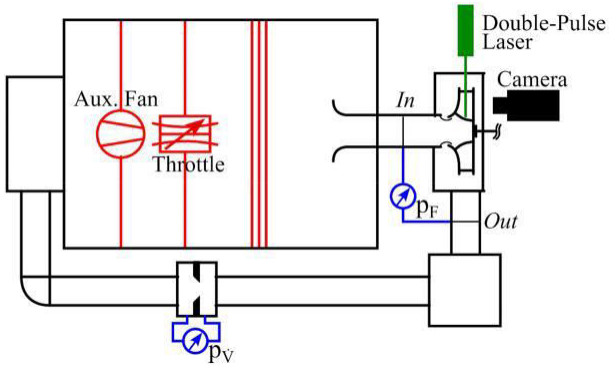

Figure 2: Experimental setup of the centrifugal test rig.

Additionally, temperature sensors are placed both in the inlet and in the outlet section close to the fan, as well as in the laboratory so as to calculate the air density. The working point can be shifted along the performance curve by either closing the throttle or powering the auxiliary fan. The inlet section of the test fan was designed to allow for simple boundary conditions for the numerical simulations.

2.3 Modelling

The unsteady CFD flow simulations provide in-depth information regarding both aerodynamics and aeroacoustics. Direct numerical simulation (DNS) methods solve the Navier–Stokes equation without any simplifications and predict the unsteady flow including all fluctuations in space and time, and thereby – the acoustic field. Unfortunately, such methods are very demanding in terms of computational time and are not available for technical applications at the moment. Similarly, large eddy simulation (LES) methods are not practical for those applications either, because the requirement regarding the numerical mesh resolution is extremely difficult to meet. Therefore, only the unsteady Reynolds-averaged Navier–Stokes (URANS) methods are left to be considered herein as a tool for CFD modelling. It is known that

URANS solutions do not capture the correct spectrum of spatial and time scales in the flow. A partial remedy for that can be the use of hybrid methods, e.g. the detached eddy simulation (DES = URANS+LES) or advanced turbulence models, such as the scale adaptive simulation (SAS) [17]. The SAS concept is based on the introduction of the von Karman length scale into the turbulence scale equation. The information provided by the von Karman length scale allows SAS models to dynamically adjust to resolved structures in the URANS simulation, which results in an LES-like behaviour in the flow unsteady regions. In the presented CFD simulations of the unsteady flow in the centrifugal fan available in the Ansys CFX commercial code [18], the URANS method with the SAS-SST and shear stress transport (SST) turbulence models will be used and compared. The advantage of the SAS-SST turbulence model will be demonstrated in capturing the unsteady fluctuations that can be treated as acoustic sources, which was already proven in our previous papers [4].

The computation domain is split into two parts, where the flow field in the volume containing the fan blades is computed in a rotating frame, and the inlet and the discharge duct are set as stationary (Fig. 3).

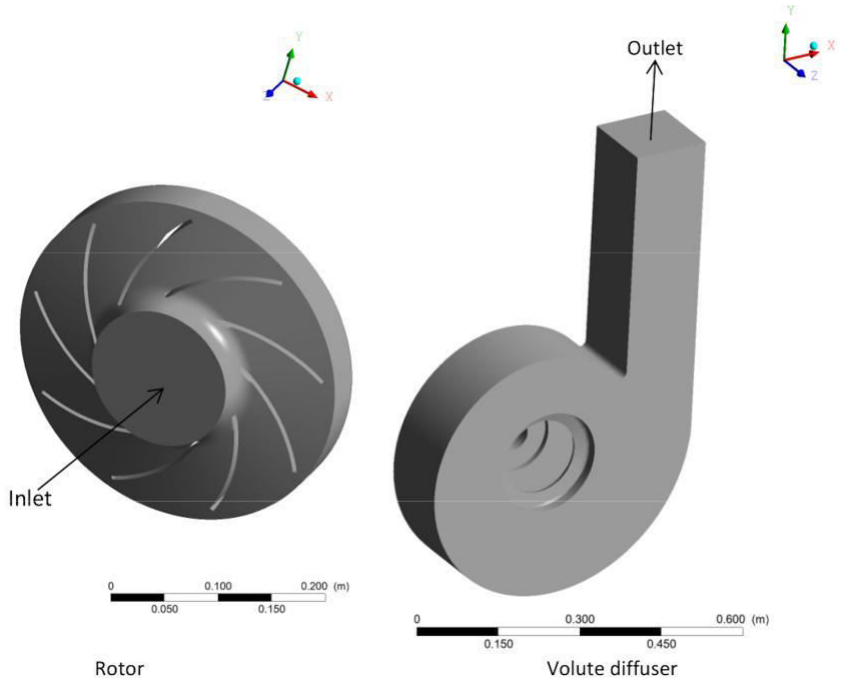

Figure 3: Computational domains of the centrifugal fan.

The unsteady time-dependent flow was solved using a second-order back-ward Euler scheme with the time step of 1×10^{-5} s, which should be small enough to allow the simulations to accurately predict frequencies up to ap-proximately 10 kHz, although the frequency range is also limited by the mesh spacing. The boundary conditions for the transient simulations were selected for the fan nominal load, i.e. the volume flow rate of 0.0637 kg/s. This value was set up at the outlet, whereas at the inlet total parameters were assumed, i.e. total pressure of 1 bar and total temperature of 300 K. The rotor rotational speed is 600 rpm. The simulations are conducted on a coarse and a fine mesh, which is described in the section devoted to pre-sentations of the results.

3 Characteristics – validation of the CFD method

The operating range of fans is limited by flow instabilities at low mass-flow rates (e.g. rotating stall or surge). Figure 4 shows the fan characteristics as the relationships between the pressure rise, efficiency and the volume flow rate for the rotor constant speed (600 rpm), obtained experimentally and from steady-state CFD simulations with the SST turbulence model on the coarse mesh. It can be noticed that there is a very good convergence between the experimental and numerical results. This means that, qualitatively, the adopted numerical method well captures the operating conditions of the centrifugal fan under consideration.

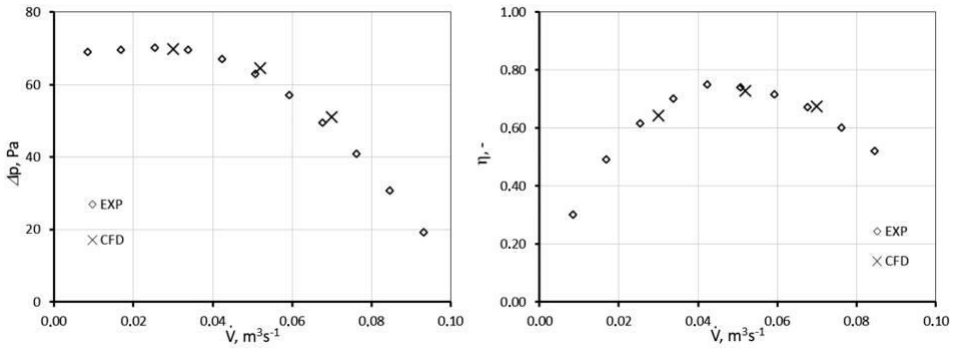

Figure 4: Fan characteristics – comparison of the experiment with CFD modelling.

4 CFD/CAA results

4.1 Coarse numerical mesh

The numerical mesh for the case under analysis contains about 0.65 × 10^6 nodes for the rotor domain and 0.8 × 10^6 for the stator domain, which gives almost 1.5 × 10^6 nodes in total. The numerical mesh is of a tetrahedral type with prisms in boundary layers. The y^+ value ranged from 1 for the rotor blades to 3 for the outlet part of the diffuser. Figure 5 shows the absolute velocity distribution at the plane perpendicular to the axis in the middle span of the rotor blades. A repeatable flow structure can be observed between the blades for the results of the URANS method with the SST turbulence model, while for the results obtained using the SAS turbulence model, the flow structure is more irregular.

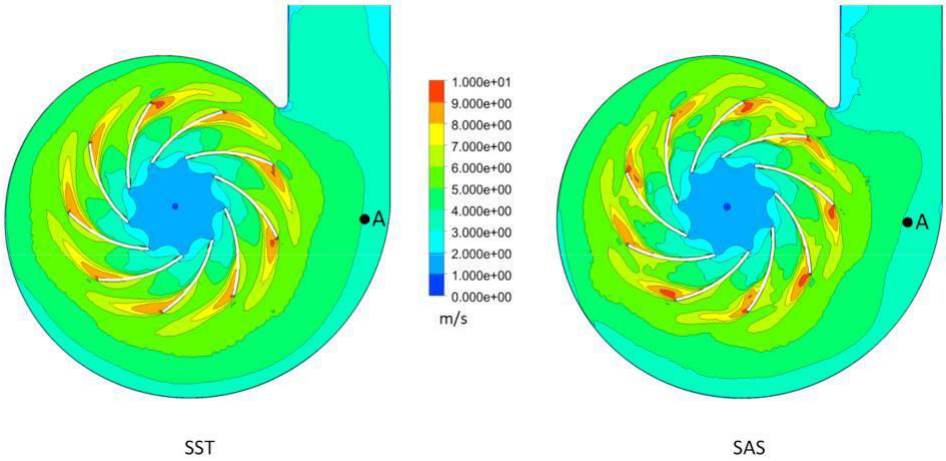

Figure 5: Absolute velocity distributions in the XY plane.

The unsteadiness features, i.e. frequency and amplitude, were identified by means of the fast Fourier transform (FFT) analysis. For this purpose, a few control points were selected in the flow domain. In this paper, the FFT results are compared for a single point located in the impeller out-let area (position A in Fig. 5). The results of the FFT analysis for this point are presented in Fig. 6, which shows acoustic pressure as a function of frequency. The maximum amplitude of the pressure fluctuations is about 0.7 Pa and corresponds to the blade passing frequency (BPF) and its harmonics. The BPF obtained from the URANS simulations with the SST

and the SAS turbulence model totals 97 Hz, which seems to be a bit too high. In the result of the simulation based on the SAS turbulence model, there is a frequency that is half the BPF value. Additionally, significant differences appear between the two models for higher frequencies, exceed-ing 1.5 kHz.

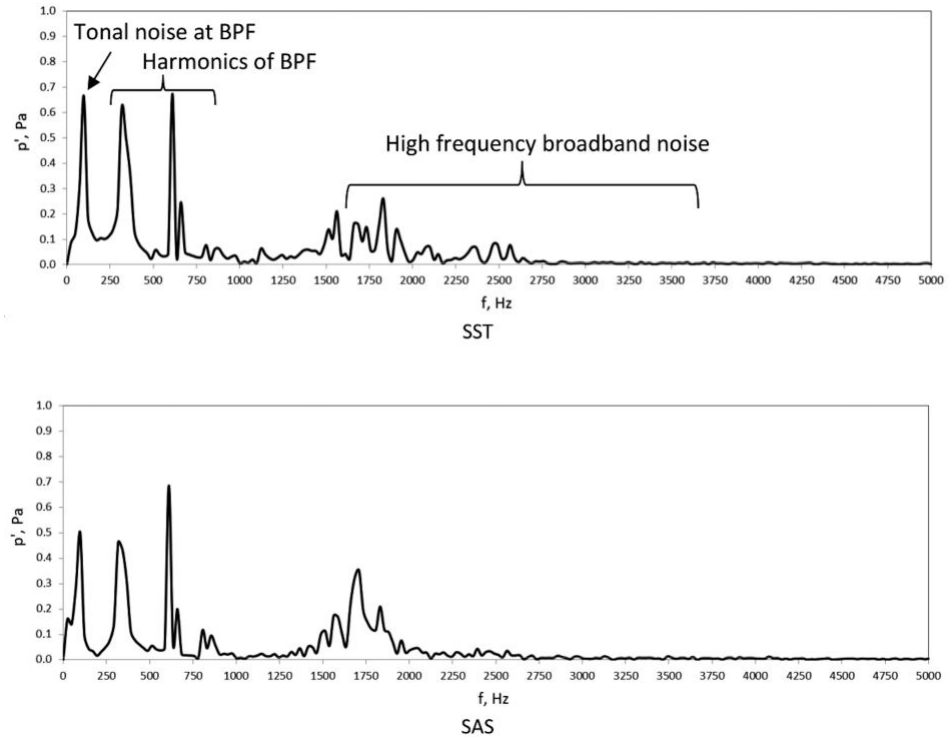

Figure 6: Fast Fourier transform analysis in point A.

4.2 Fine numerical mesh

As the URANS method with the SAS turbulence model performs well in capturing the unsteady effects, especially in blade-to-blade channels, a de-cision was made to carry out the simulations with the same turbulence model on a twice denser numerical grid. The total number of nodes of the numerical grid in this case slightly exceeded 3×10^6.

Figure 7 gathers the data of the absolute velocity distribution and the FFT analysis results for the point mentioned above. Looking at the ab-solute velocity distribution, smaller spatial scales can be identified, due

to the much finer mesh. Unfortunately, the time scales are limited by the time step used in the simulation. The time step assumed for the fine mesh was the same as for the coarse one: $\Delta t = 10^{-5}$ s. A much smaller time step was required, but it would have lengthened the computational time dramatically. The FFT analysis revealed a new frequency in the vicinity of the BPF and its harmonics. Also, the acoustic pressure amplitude rises to 1 Pa.

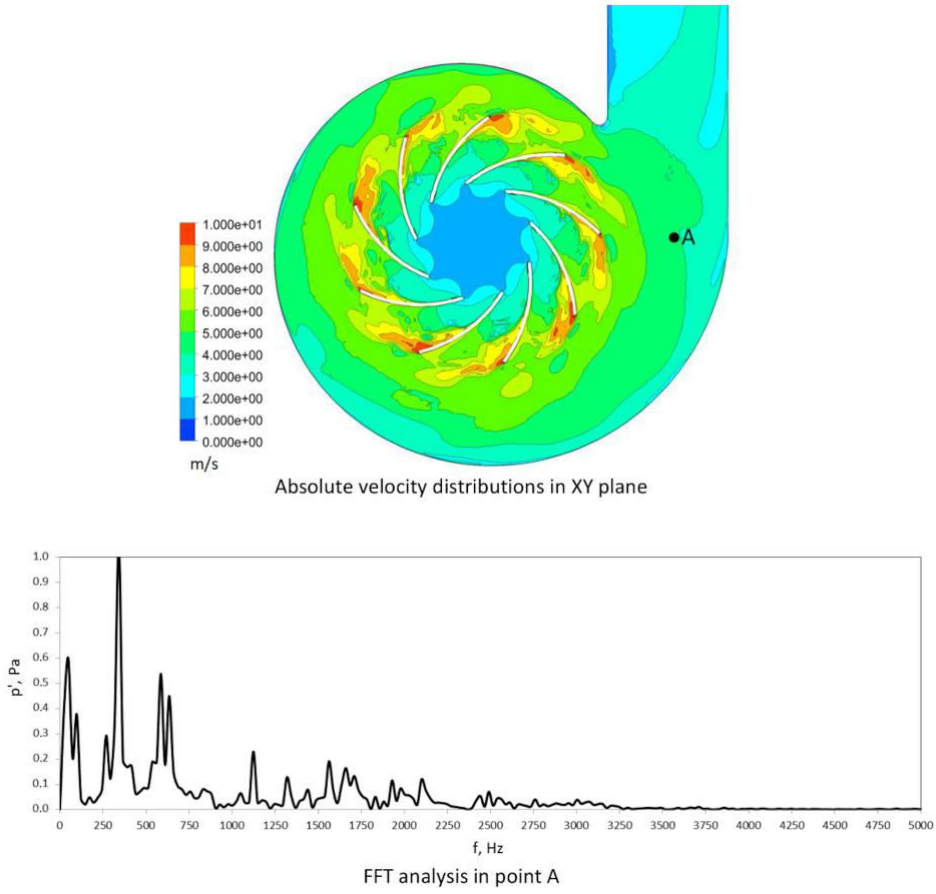

Figure 7: CFD results for the fine mesh.

Figure 8 presents the acoustic wave propagations out of the impeller. Small structures can be seen between the rotor blades and the acoustic wave corresponding to the low frequency, related to the BPF.

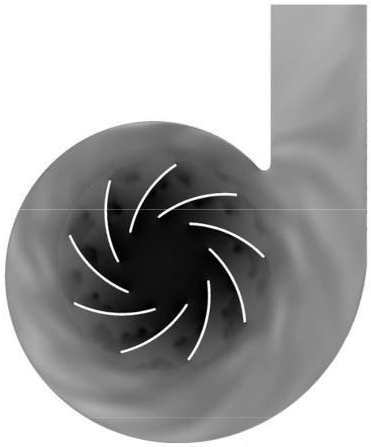

Figure 8: Acoustic wave propagation in the fan.

5 Conclusions

This paper presents the results of a collaboration recently started between the Institute of Thermal Turbomachinery of the Karlsruhe Institute of Technology and the Department of Power Engineering and Turbomachin-ery of the Silesian University of Technology to investigate the flow field within a centrifugal fan. The research is both experimental and numerical. The first step was to establish the research methodology.

The presented CFD results show that the URANS method with the SST turbulence model predicts the analysed fan operating conditions. All the presented unsteady CFD simulations capture the BPF and its harmonics well. However, using the SAS turbulence model, valuable results are ob-tained in wide spectra of frequencies. Based on that information, further experiments will be planned to measure acoustic pressure and use these data to validate the CFD method. This will enable quantitative determi-nation of the applied CFD method of modelling acoustic characteristics of fans. Moreover, the planned PIV measurements will provide valuable data for the validation of CFD methods.

As it is known, the small centrifugal fan analysed herein was designed to work well under nominal load conditions. However, due to the interaction with the piping system, temporary drops in the flow rate may appear. Therefore, further numerical and experimental efforts will be made to study the onset of a stall, which has a fundamental effect on the safety of the device operation.

Acknowledgement The numerical part of the presented research was supported by the Silesian University of Technology within the Initiative of Excellence – Research University programme (08/050/SDU20/10-2703) and co-financed by the European Union through the European Social Fund (POWR.03.05.00-00-Z305).

Received 3 June 2021

References

[1] Dykas S., Wróblewski W., Rulik S., Chmielniak T.: *Numerical method for modelling of acoustic waves propagation*. Arch. Acoust. **35**(2010), 1, 35–48.

[2] Fortuna S., Sobczak K.: *Numerical and experimental investigations of the flow in radial fan*. Mechanics **27**(2008), 4, 138–143

[3] Moon Y.J., Cho Y., Nam H.S.: *Computation of unsteady viscous flow and aeroacoustic noise of the cross flow fan.* Comput. Fluids **32**(2003), 7, 995–1015.

[4] Rulik S., Dykas S., Wroblewski W.: *Modelling of aerodynamic noise using hybrid SAS and DES methods*. In: Proc. ASME Turbo Expo 2010: Power for Land, Sea and Air, Glasgow, June 14–18, 2010, **7**(2010), 2835–2844., GT2010-2269.

[5] Stasko T., Dykas S., Majkut M., Smolka K.: *An attempt to evaluate the cy-cloidal rotor fan performance*. Open J. Fluid Dynam. **9**(2019), 4.

[6] Benedek T., Vad J.: *Beamforming based extension of semi-empirical noise modelling for low-speed axial flow fans*. Appl. Acoust. **178**(2021), 108018.

[7] Jiang H., Wang Q., Zheng T.F., Tu C.X., Zhang K.: *PIV measurement of internal flow field in a range hood*. In: Energy and Mechanical Engineering (S.Y. Liang, Ed.), 2015 Int. Conf. on Energy and Mechanical Engineering, Wuhan, 17-18 Oct. 2015, World Scientific, 2016, 570–575.

[8] Probst M., Pritz B.: *Quantitative validation of CFD-simulation against PIV data for a centrifugal fan*. In: Proc. 14th Int. Symp. on Experimental Computational Aerothermodynamics of Internal Flows, Gdańsk 8-11 July 2019.

[9] Neise W., Michel U.: *Aerodynamic Noise of Turbomachines*. DLR-Interner Bericht, Berlin 1994.

[10] Jeon W.H., Lee D.J., Rhee H.: *An application of the acoustic similarity law to the numerical analysis of centrifugal fan noise*. JSME Int. J. C-mech Sy. **47**(2004), 3, 845–851.

[11] Kissner C., Guerin S.: *Comparison of predicted fan broadband noise using a two- versus a three-dimensional synthetic turbulence method*. J. Sound Vib. **508**(2021), 116221.

[12] Jaron R., Herthum H., Franke M., Moreau A., Guerin S.: *Impact of turbu-lence models on RANS-informed prediction of fan broadband interaction noise*. In: Proc. 12th Eur. Turbomachinery Conference (ETC), Stockholm, 3-7 April, 2017.

[13] Carolus T.: *Theoretische und experimentelle Untersuchung des Pumpens von luft-technischen Anlagen mit Radialventilatoren*. PhD thesis, Karlsruhe University of Applied Sciences, Karlsruhe 1984.

[14] Blazquez-Navarro R., Corral R.: *Prediction of fan acoustic blockage on fan/outlet guide vane broadband interaction noise using frequency domain linearized Navier–Stokes solvers.* J. Sound Vib. **508**(2021), 116033.

[15] Ffowcs-Williams J.E., Hawkings D.L.: *Sound generation by turbulence and sur-faces in arbitrary motion.* Philos. T.R. Soc. Lond. S-A, **264**(1969), 1151, 321–342.

[16] Lighthill M.J.: *On sound generated aerodynamically. I. General theory*. Proc. R. Soc. Lon. Ser.-A **211**(1952) 1107, 564–587

[17] Menter F.R., Egorov Y.: *A scale-adaptive simulation model using two-equation models*. In: Proc. 43th AIAA Aerospace Sciences Meeting and Exhibit, Reno, 10-13 Jan. 2005, AIAA 2005-1095.

[18] Ansys Fluent Theory Guide, 2021R1. https://www.ansys.com (acessed 1 July 12021).